JOURNAL OF SYNCHROTRON RADIATION
ISSN 1600-5775

Minimizing experimental artefacts in synchrotron-based X-ray analyses of Fe speciation in tissues of rice plants

Peng Wang,[a,b]* Brigid A. McKenna,[b] Neal W. Menzies,[b] Cui Li,[b] Chris J. Glover,[c] Fang-Jie Zhao[a] and Peter M. Kopittke[b]

[a]College of Resources and Environmental Sciences, Nanjing Agricultural University, Nanjing, 210095, People's Republic of China, [b]School of Agriculture and Food Sciences, The University of Queensland, St Lucia, Queensland 4072, Australia, and [c]Australian Synchrotron ANSTO, Clayton, Victoria 3168, Australia. *Correspondence e-mail: p.wang3@njau.edu.cn

Received 13 December 2018
Accepted 30 March 2019

Edited by R. W. Strange, University of Essex, UK

Keywords: X-ray absorption spectroscopy; iron speciation; photoreduction; beam damage; cryostats; freeze drying; plant-root tissues.

Iron (Fe) plays an important role within environmental systems. Synchrotron-based X-ray approaches, including X-ray absorption spectroscopy (XAS), provide powerful tools for *in situ* analyses of Fe speciation, but beam damage during analysis may alter Fe speciation during its measurement. XAS was used to examine whether experimental conditions affect the analysis of Fe speciation in plant tissues. Even when analyzed in a cryostat at 12 K, it was found that Fe^{III} can rapidly (within 0.5–1 min) photoreduce to Fe^{II}, although the magnitude of photoreduction varied depending upon the hydration of the sample, the coordination chemistry of the Fe, as well as other properties. For example, photoreduction of Fe^{III} was considerably higher for aqueous standard compounds than for hydrated plant-root tissues. The use of freeze-dried samples in the cryostat (12 K) markedly reduced the magnitude of this Fe^{III} photoreduction, and there was no evidence that the freeze-drying process itself resulted in experimental artefacts under the current experimental conditions, such as through the oxidation of Fe^{II}, although some comparatively small differences were observed when comparing spectra of hydrated and freeze-dried Fe^{II} compounds. The results of this study have demonstrated that Fe^{III} photoreduction can occur during X-ray analysis, and provides suitable conditions to preserve Fe speciation to minimize the extent of beam damage when analyzing environmental samples. All studies utilizing XAS are encouraged to include a preliminary experiment to determine if beam damage is occurring, and, where appropriate, to take the necessary steps (such as freeze drying) to overcome these issues.

1. Introduction

Synchrotron-based X-ray approaches, including X-ray absorption spectroscopy (XAS), are valuable in examining elemental speciation within a wide variety of materials, including plant tissues and environmental samples. For example, XAS offers a range of advantages compared with other approaches for examining elemental speciation, perhaps the most important of which is the ability to examine samples *in situ*. Accordingly, XAS has been used to examine a wide range of environmental samples, including plant tissues (Castillo-Michel *et al.*, 2017; Wang *et al.*, 2017), soils and sediments (Burton *et al.*, 2009; Wang *et al.*, 2018; Wu *et al.*, 2018), and in aquatic samples (Bai *et al.*, 2016; von der Heyden *et al.*, 2014).

Of particular interest in the present study is Fe, which is the fourth most abundant element in the earth's crust and soil (Sposito, 2008), is an essential nutrient for plants and animals, and has important roles in aquatic ecosystems. Iron has a range of oxidation states (of which both Fe^{II} and Fe^{III} are

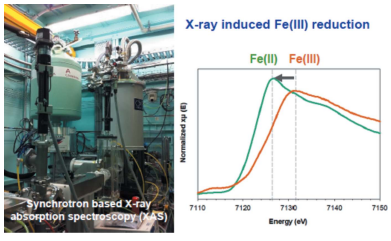

commonly found in environmental systems), and hence understanding the speciation of Fe within environmental systems is critical in understanding its behaviour and function. In this regard, synchrotron-based XAS analyses have been used to investigate a wide range of Fe-containing processes, including the oxidation of Fe in acid sulfate sediments (Morgan *et al.*, 2009), the speciation of Fe within soils (Prietzel *et al.*, 2007) and minerals (Shorttle *et al.*, 2015), its speciation in waste materials including mine tailings (Essilfie-Dughan *et al.*, 2017; Hayes *et al.*, 2014), its speciation in aquatic ecosystems (Bai *et al.*, 2016; von der Heyden *et al.*, 2014), as well as the form of Fe within plant tissues and the associated human food products (De Brier *et al.*, 2016; Terzano *et al.*, 2013; Yoshimura *et al.*, 2000). The speciation of Fe within plant tissues is of particular importance, for example, given that Strategy I and Strategy II plants differ in their approach for the acquisition of Fe, either as Fe^{II} or as Fe^{III} (Marschner & Römheld, 1994).

Despite its usefulness, it is known that X-ray beams can also cause damage to the sample, resulting in experimental artefacts (George *et al.*, 2012). This is especially important when examining the speciation of Fe which is known to be particularly redox sensitive. For example, Terzano *et al.* (2013) conducted a study to determine the speciation of Fe in the sap of tomato (*Solanum lycopersicum* L.), and found that Fe^{III} in the samples can be photoreduced from Fe^{III} to Fe^{II} during analysis. In a similar manner, Sigfridsson *et al.* (2013) demonstrated the photoreduction of Fe in enzymes during X-ray analyses. In contrast, other authors have reported that no photoreduction of Fe was observable under their experimental conditions (Grillet *et al.*, 2014; James *et al.*, 2016). However, perhaps most importantly, many studies examining Fe using X-ray based approaches in environmental investigation do not appear to explicitly consider the issue of beam damage (including photoreduction), with their findings potentially confounded by experimental artefacts.

The aim of the present study was to examine the experimental conditions that are suitable for the examination of Fe speciation using synchrotron-based X-ray analyses. We aimed to (i) highlight the types of problems associated with beam damage in X-ray studies of Fe, (ii) examine the factors which influence the severity of this beam damage and (iii) broadly provide information on the types of approaches which can be used to overcome these problems. For this study, we utilized XAS analyses, including both X-ray absorption near-edge structure (XANES) spectroscopy and extended X-ray absorption fine structure (EXAFS). However, the concepts developed in the present study also apply to other X-ray approaches, including μ-XANES analyses at X-ray fluorescence microscopy (XFM) beamlines. We have focused on the examination of root tissues of rice plants as examples of 'environmental' samples, with these roots being highly hydrated (>95% water) and hence possibly more susceptible to beam damage than other types of samples. It is important to note that Fe is particularly redox sensitive, and studies investigating other metal(loid)s, such as Zn and Cd, are less likely to encounter issues with beam damage during XAS analyses as examined in the present study.

2. Materials and methods

2.1. Plant growth

Seeds of rice (*Oryza sativa* L.) were surface sterilized with 8% NaClO and rinsed using sterile water before being germinated in rolled paper towel suspended in tap water. After 4 days, the seedlings were transferred to containers with 11 l of nutrient solution (μ*M*): 680 NO_3^-–N, 120 NH_4^+–N, 100 Ca, 100 Mg, 310 K, 350 SO_4^{2-}–S, 10 P, 25 Fe (supplied as Fe^{III}EDTA; EDTA: ethylenediaminetetraacetic acid), 3.0 B, 1.0 Mn, 0.05 Cu, 1.0 Zn and 0.02 Mo. The pH of the continuously aerated nutrient solutions was not adjusted (*ca* pH 5.6). Plants were grown at 25°C with 14 h of light at a photon flux density of 400 μ*M* m^{-2} s^{-1}. All nutrient solutions were renewed every 2 days. After 7 days, the roots were washed with flowing deionized water before the plants were separated into roots and shoots. Root tissues were snap frozen in liquid nitrogen for later analysis using XAS, with approximately half of these frozen root tissues maintained in liquid nitrogen whilst the other half were freeze dried. In addition, a further sub-sample of the root tissues was dried (65°C) and digested in a 1:5 mixture of nitric acid and perchloric acid and analyzed using inductively coupled plasma mass spectroscopy to determine the bulk Fe concentration of the root tissue. The average bulk Fe concentration of the root tissues was determined to be 20.3 mg kg^{-1} on a fresh-mass basis and 304 mg kg^{-1} on a dry-mass basis (93% water content).

2.2. XAS analyses

All analyses were undertaken at the XAS beamline at the Australian Synchrotron (Melbourne, Australia). The use of this beamline to examine environmental samples has been described previously (Kopittke *et al.*, 2011). The XAS beamline utilizes a 1.6 T wiggler, Si collimating mirror cryo-cooled Si(111) monochromator and Rh-coated torodial refocusing mirror. The X-ray beam spot at the sample was set at *ca* 2 mm × 0.3 mm (H × V), which was defocused. The flux was determined to be 1.5×10^{12} photons s^{-1}, resulting in a flux density of *ca* 3×10^{12} photons s^{-1} mm^{-2}. Under the current experimental conditions, this was calculated as corresponding to a dose of 5.4×10^3 Gray s^{-1}. The energy scale was calibrated by the simultaneous measurement of a metallic Fe reference foil in transmission. Under the experimental conditions of this experiment, the energy scale was typically stable to 0.05 eV or better. Fluorescence spectra were measured with a 100-element solid-state detector at 90° to the incident beam. The samples were analyzed *in situ* using the Fe *K* edge (7112 eV) using both XANES and EXAFS. All samples, whether hydrated or freeze dried, were analyzed in a He exchange gas cryostat at a temperature of *ca* 12 K.

A range of samples and standard compounds were prepared for analyses using XAS. Where dehydrated (freeze-dried) plant-tissue samples were used, these were ground at room temperature using an agate ball mill grinder. The fine powder was then prepared into a pellet using a manual pellet press before being placed in a Perspex sample holder sealed with

Kapton tape. For plant-tissue samples that were hydrated (frozen), the plant tissues were placed into an agate mortar and pestle and ground under liquid nitrogen before being placed in a sample holder, sealed with Kapton tape, and transferred directly to the cryostat (12 K). Thus, for the frozen plant tissues, the samples were never permitted to thaw prior to analysis. The plant-tissue samples, both hydrated (frozen) and dehydrated (freeze dried), were then analyzed as outlined below.

A total of five different Fe-containing standard compounds were prepared for XAS analysis. These compounds consisted of four Fe^{III} standards plus four Fe^{II} standards. The four Fe^{III} and Fe^{II} standards had an Fe concentration of 3.6 m*M* (200 mg l^{-1}), being prepared with either $Fe_2(SO_4)_3$ or with $FeSO_4$. For both Fe^{III} and Fe^{II}, the final standard mixtures consisted of (i) 3.6 m*M* Fe, and (ii–iv) 3.6 m*M* Fe mixed with 36 m*M* of one of three ligands (citric acid or phytic acid, and cysteine). The ligand was provided at a concentration ten times higher than the metal to maximize the binding of the Fe to the ligand. For all eight of these Fe^{III} and Fe^{II} standards, the solutions were either prepared in ambient conditions or inside an O_2-free glovebox (LC Technology Solutions, USA) as described later. For the solutions where the Fe was mixed with other ligands (citric acid or phytic acid, and cysteine), solution pH was adjusted to *ca* 5.5 using 0.1 *M* NaOH. The pH of the Fe^{III} sulfate and Fe^{II} sulfate solutions was not adjusted. A pH of 5.5 was selected as this is similar to values encountered in relevant plant cellular compartments, such as the vacuole. After preparation, these five standards were either directly utilized (*i.e.* hydrated, albeit frozen once placed in the cryostat) or they were first freeze dried. Where samples were analyzed hydrated, they also contained 30% glycerol to reduce ice-crystal formation during cooling (initial concentrations of Fe were adjusted so that the final Fe concentrations remained 3.6 m*M*). For the standards that were analyzed as solutions, the time from preparation to analysis was less than 30 min. Where the freeze-dried standard compounds were examined, they were first diluted by mixing with cellulose to achieve a final concentration of *ca* 200 mg kg^{-1}.

Experiment 1 aimed to determine whether the presence of O_2 during sample preparation resulted in the oxidation of Fe^{II}. For this experiment, XANES and EXAFS spectra were obtained for Fe^{II} sulfate solutions that had been prepared either in ambient conditions or in an O_2-free glove box. Two replicate scans were performed on both of the standards, with the total exposure time being 600 s per scan. To minimize the risk of beam damage, the two replicate scans were performed at different locations on the sample (*i.e.* the sample position was moved between the two scans).

Experiment 2 examined whether the freeze-drying process resulted in a change in Fe speciation. First, two standard compounds were examined, being an Fe^{II} sulfate solution that was examined hydrated (frozen) plus the corresponding solution that had been freeze dried. In addition, two plant-root samples were examined, again being a hydrated (frozen) sample plus the corresponding freeze-dried sample. Samples were scanned as outlined above.

Experiment 3 aimed to determine the extent to which Fe^{III} is photoreduced during analysis. Three samples were examined, being the Fe^{III} sulfate solution, a freeze-dried Fe^{III} sulfate standard, and the Fe^{II} sulfate solution. First, a normal XANES and EXAFS scan was performed for all three compounds as described earlier. Next, to provide a detailed analysis of the rate at which Fe^{III} photoreduction occurs, a different type of scan was performed in which the energy of the incident X-rays was maintained constant. In this regard, by carefully selecting the energy, it was possible to determine the speed (and extent) of the photoreduction of Fe^{III}. Specifically, we selected two individual energy values (7126.1 and 7131.0 eV) for study. The first of these energy values (7126.1 eV) corresponds to the white line peak where the spectrum for Fe^{II} compounds have the highest fluorescence intensity and thus the photoreduction of Fe^{III} to Fe^{II} would be associated with a concomitant increase in fluorescence intensity at 7126.1 eV (see spectra in *Results* for further illustration). The second value (7131.0 eV) corresponds to the white line peak for Fe^{III} compounds [where Fe^{III} compounds have a higher fluorescence intensity than Fe^{II} compounds] and thus the photoreduction of Fe^{III} to Fe^{II} would be associated with a concomitant decrease in fluorescence intensity. At these two energy values, fluorescence intensity was measured every 0.4 s across a total exposure time of 300 s.

Experiment 4 examined whether the rate of Fe^{III} photoreduction was influenced by the ligand to which the Fe^{III} was bound. A total of nine samples were examined. For Fe^{III}, the citrate, phytate and cysteine standards were examined, both as hydrated and as freeze-dried samples (yielding a total of six Fe^{III} standards). For Fe^{II}, we also examined the citrate, phytate and cysteine standards, but only as hydrated (not freeze dried). For these samples, we conducted both a normal scan, as well as examining changes in fluorescence intensity while holding energy constant at the two values as described for Experiment 3. For the scans at constant energy, we examined only the three hydrated (frozen) Fe^{III} standards.

Experiment 5 examined the potential photoreduction in roots of rice. For this experiment, we examined both hydrated (frozen) and freeze-dried sample of the roots. As described in Experiment 3, we examined changes in fluorescence intensity at two constant values for energy (7126.1 and 7131.0 eV).

The spectra were energy normalized using the reference energy of the foil, with replicate spectra merged using *Athena* 0.8.056 (Ravel & Newville, 2005).

3. Results

3.1. Oxidation of Fe^{II} during sample preparation

Our first aim (Experiment 1) was to determine if Fe^{II} compounds were likely to oxidize to Fe^{III} during their initial preparation. For this, we chose an Fe^{II} sulfate solution which we considered to be the most susceptible to oxidation. However, it was evident from both the XANES and EXAFS analyses that the method of preparation did not influence speciation (Fig. 1). Regardless of whether samples were

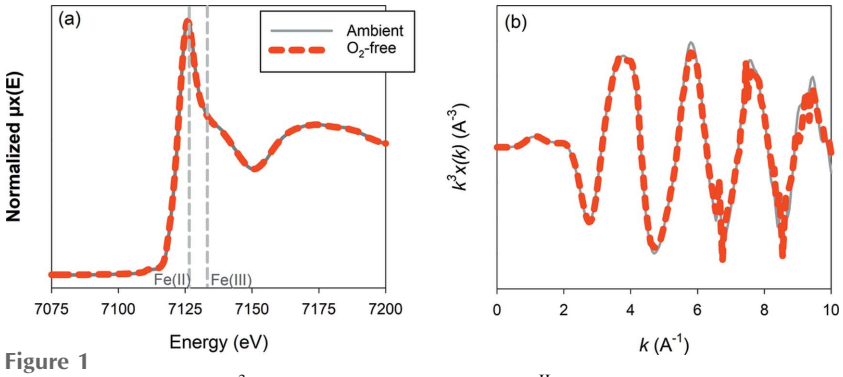

Figure 1
Fe *K*-edge XANES and k^3-weighted EXAFS spectra of Fe^{II} sulfate solution (Experiment 1). The standard was prepared either in ambient conditions or in an O_2-free glove box. The vertical dashed lines in (*a*) correspond to the white line peaks of Fe^{II} sulfate (7126.1 eV) and Fe^{III} sulfate (7131.0 eV).

prepared in an O_2-free environment or in ambient conditions (*i.e.* atmospheric O_2 concentrations), XANES and EXAFS analyses indicated that the Fe was present as Fe^{II}. It must be noted that there is a possibility that perhaps some of the Fe^{II} did indeed oxidize to Fe^{III} during the sample preparation, but that during the subsequent X-ray scanning this Fe^{III} was rapidly photoreduced back to Fe^{II} (see later). However, we contend that if this occurred, it could have only been a comparatively small proportion of the Fe^{II} that initially oxidized to Fe^{III}, as not all Fe^{III} is photoreduced to Fe^{II} during XANES and EXAFS analyses (see later).

The observation that Fe^{II} sulfate solution was not rapidly oxidized to Fe^{III} when prepared in ambient conditions was perhaps not unexpected given that free hydrated Fe^{II} often has an oxidation half life of days to weeks, although trace quantities of $Fe(OH)_2^0$ can reduce the overall oxidation half life to a few seconds [see King (1998) and references therein]. Regardless, although the oxidation of Fe^{II} to Fe^{III} was not observed during sample preparation in the present study when prepared in ambient conditions, care should still always be taken when preparing redox-sensitive samples for analysis to avoid changes in speciation during sample preparation in order to avoid potential experimental artefacts.

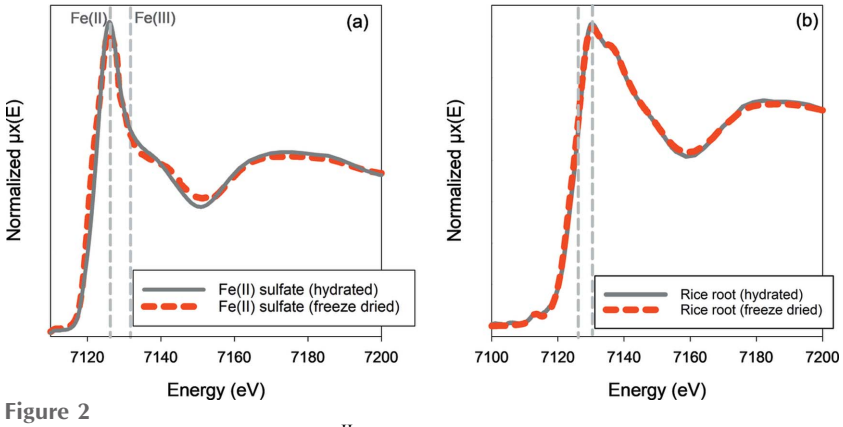

Figure 2
Fe *K*-edge XANES spectra of (*a*) Fe^{II} sulfate, either as a solution (frozen) or as a solid after freeze drying, and (*b*) rice-root tissues grown in solutions containing 25 μ*M* Fe^{III} EDTA, either hydrated (frozen) or following freeze drying (Experiment 2). The vertical dashed lines in (*a*) correspond to the white line peaks of Fe^{II} sulfate (7126.1 eV) and Fe^{III} sulfate (7131.0 eV).

3.2. Freeze drying and potential oxidation of Fe^{II}

Next, we considered whether the freeze-drying process would result in the oxidation of Fe^{II} to Fe^{III} (Experiment 2). In particular, it was of interest whether Fe^{II} would be oxidized during the preparation and drying process. We examined both a Fe^{II} sulfate solution and hydrated rice roots, and no oxidation to Fe^{III} was observed for either sample as a result of the freeze-drying process (Fig. 2). Furthermore, there was only comparatively small differences in the spectra between the hydrated and freeze-dried compounds [Fig. 2(*a*)]. Thus, when using X-ray approaches to examine Fe speciation, the data suggest that freeze drying would be suitable for sample preparation where it was not either possible or desirable to utilize hydrated samples (for example, see later).

3.3. Photoreduction of Fe^{III} and the influence of sample hydration and coordination chemistry

Given that oxidation of Fe^{II} to Fe^{III} did not appear to be of concern under the current experimental conditions (Figs. 1 and 2), we next examined whether the X-ray beam caused photoreduction of Fe^{III} (Experiment 3). First, we performed XANES and EXAFS, comparing the Fe^{III} sulfate solution, Fe^{III} sulfate solid and Fe^{II} sulfate solution [Fig. 3(*a*)]. It was found that the white line peak of the Fe^{II} sulfate solution was at 7126.1 eV, corresponding to the approximate value expected for Fe^{II} (for example, see Wilke *et al.*, 2001). In contrast, for the Fe^{III} sulfate solution, although there was a small shoulder at 7131.0 eV (corresponding to the Fe^{III} white line peak; for example, see Wilke *et al.*, 2001), the white line peak was actually at *ca* 7126 eV and was thus similar to Fe^{II} rather than Fe^{III} [Fig. 3(*a*)]. This observation was unexpected and is attributed to the comparatively rapid photoreduction of Fe^{III} to Fe^{II} in this hydrated (frozen) standard. It was apparent that much of the Fe^{III} had already been reduced to Fe^{II} by the time that the XANES scan had reached 7126 eV, with this corresponding to an exposure of *ca* 230 s to this location within the XANES scan. This photoreduction of Fe^{III} to Fe^{II} was also evident by examining the EXAFS spectra [Fig. 3(*b*)] and by examining the derivative of the XANES spectra [Fig. 3(*c*)]. Importantly, however, it was also observed that the Fe^{III} sulfate solid (freeze-dried) standard was substantially less sensitive to photoreduction, with the white line peak for this Fe^{III} compound corresponding to the expected value of 7131.0 eV and with no noticeable shoulder at 7126.1 eV [Fig. 3(*a*)].

To examine the kinetics of the photoreduction of Fe^{III} to Fe^{II} more closely, we

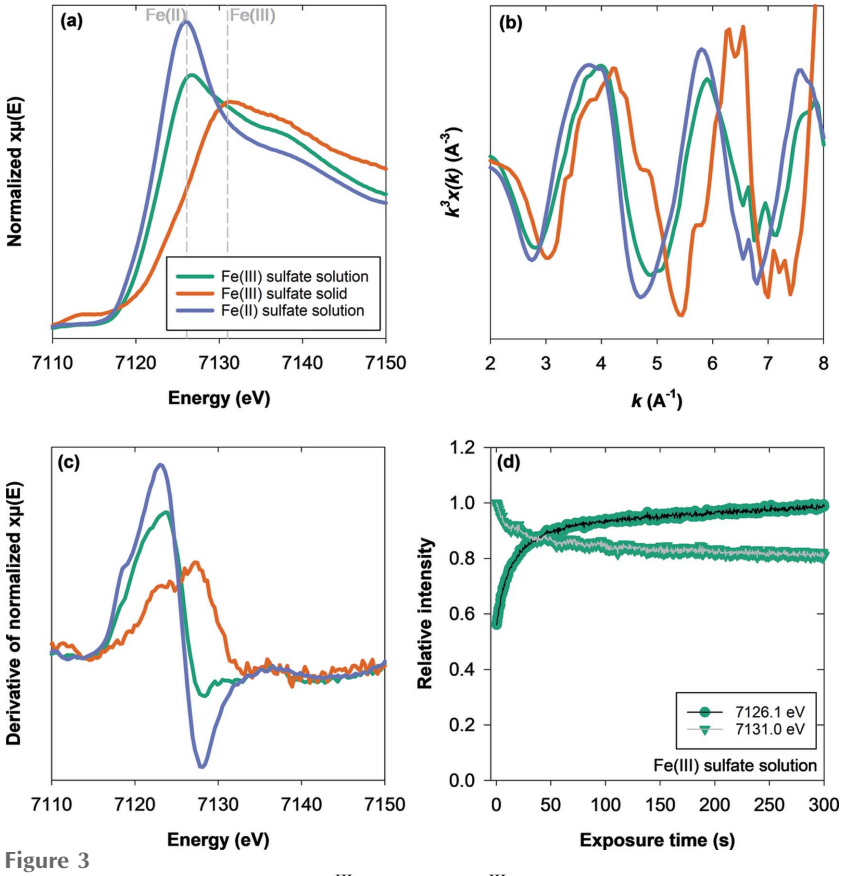

Figure 3
X-ray induced photoreduction of Fe^{III}, comparing Fe^{III} sulfate (either as hydrated or freeze-dried forms) with Fe^{II} sulfate (hydrated) (Experiment 3). (*a*) Fe *K*-edge XANES, (*b*) k^3-weighted EXAFS, and (*c*) derivative of normalized XANES. In (*d*), a hydrated (frozen) Fe^{III} sulfate sample was scanned at constant energy corresponding to the white line peaks of Fe^{II} and Fe^{III} sulfates (7126.1 or 7131.0 eV) for 300 s. At 7126.1 eV, a progressive increase in fluorescence intensity would correspond to the conversion of Fe^{III} to Fe^{II} (and *vice versa*), while at 7131.0 eV, a progressive increase in fluorescence intensity would correspond to the conversion of Fe^{II} to Fe^{III} (and *vice versa*).

measured changes in fluorescence intensity over time whilst scanning at a constant energy of either 7126.1 or 7131.0 eV (these values corresponding to the white line peaks of Fe^{II} and Fe^{III}, respectively). Thus, at these constant energy values, a change in fluorescence intensity would correspond to a change in Fe speciation. Specifically, at 7126.1 eV the photoreduction of Fe^{III} would cause an increase in fluorescence intensity, whilst at 7131.0 eV the photoreduction of Fe^{III} would cause a decrease in fluorescence intensity [compare the XANES spectra in Fig. 3(*a*)]. From these analyses, it was apparent that the extent of Fe^{III} photoreduction in the hydrated Fe^{III} standard was both substantial and rapid, with the majority of photoreduction occurring within 0.5–1 min of exposure [Fig. 3(*d*)].

Next, we examined whether the rate of photoreduction was also influenced by the ligand to which the Fe^{III} was bound (*i.e.* coordination chemistry). Specifically, we found that the rate of photoreduction was greatest for free Fe^{III} ions (*i.e.* the Fe^{III} sulfate solution), followed by Fe^{III} complexed with phytate and citrate (cysteine is considered later) (Figs. 3 and 4). Thus, when conducting preliminary studies to determine whether photoreduction (beam damage) is of concern within a particular experimental system, care should be taken to ensure that the most sensitive sample is examined. It was interesting to note that the photoreduction of Fe^{III} within the highly hydrated plant-root tissues was negligible (Fig. 5) despite the Fe being present as Fe^{III} [Fig. 2(*b*)], suggesting that the sample properties influence the magnitude of the beam damage.

3.4. Reduction of Fe^{III} by cysteine

For Fe^{III} cysteine, it was noted that all three XANES spectra had white line peaks that corresponded to Fe^{II} [Fig. 4(*e*)] and that there was no change in fluorescence intensity over time when measured at constant energy [Fig. 4(*f*)]. Thus, the data suggest that the Fe in all three samples was already present as Fe^{II} at the commencement of XAS analyses. We suggest that this is probably because of the reduction of Fe^{III} by cysteine itself (which is a reducing agent) upon sample preparation. For example, cysteine has been reported to cause the reductive dissolution of Fe^{III} (Doong & Schink, 2002). Thus, these data demonstrate that care must be taken when analyzing and interpreting cysteine standards prepared using Fe^{III}, as the Fe^{III} would potentially have been reduced to Fe^{II}.

3.5. Implications for study of plant tissues

The results of the present study have implications for reducing the formation of experimental artefacts during X-ray analyses of Fe speciation in environmental samples. Most importantly, we have shown that in comparatively high-flux beamlines (such as the XAS beamline at the Australian Synchrotron), hydrated samples are susceptible to rapid photoreduction of Fe^{III} to Fe^{II}, with much of this occurring within only 0.5–1 min of exposure [Fig. 3(*d*)]. By using freeze-dried samples rather than hydrated samples, it was found that the rate of the photoreduction of Fe^{III} to Fe^{II} decreased markedly [Figs. 3(*a*), 4(*a*) and 4(*c*)]. Interestingly, however, the photoreduction of Fe^{III} within hydrated plant-root tissues was negligible (Fig. 5) despite the Fe being present as Fe^{III} [Fig. 2(*b*)], confirming that the sample properties influence the likelihood of beam damage in any given experiment.

Not only did the hydration of samples influence the rate of the photoreduction of Fe^{III}, but the coordination chemistry of the Fe^{III} was also important. For example, it was found that the photoreduction of Fe^{III} decreased in the order: free Fe^{3+} ions (Fe^{III} sulfate solution) > Fe^{III} phytate > Fe^{III} citrate (Fig. 4). We have also confirmed that in the present experimental conditions the process of freeze-drying hydrated standards and plant tissues did not result in oxidation of Fe^{II} to Fe^{III}

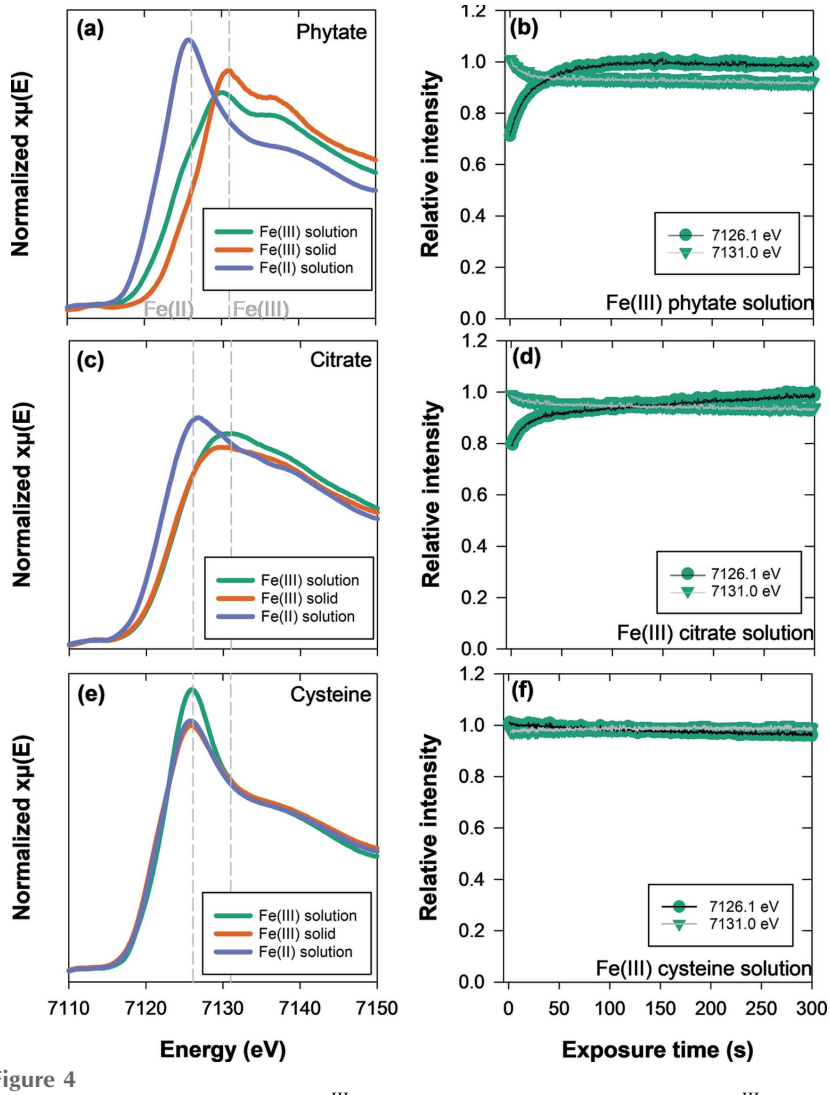

Figure 4
X-ray induced photoreduction of Fe^{III} as influenced by chelation, comparing Fe^{III} and Fe^{II} chelated with phytate (*a*, *b*), citrate (*c*, *d*) or cysteine (*e*, *f*) (Experiment 4). Both hydrated and freeze-dried forms were compared. (*a*), (*c*), (*e*) Fe *K*-edge XANES spectra of the Fe^{III} complex (hydrated and freeze dried) compared with the Fe^{II} complex (hydrated). In (*b*, *d*, *f*), hydrated (frozen) Fe^{III} samples complexed with (*b*) phytate, (*d*) citrate and (*f*) cysteine, were scanned at constant energy corresponding to the white line peaks of Fe^{II} and Fe^{III} sulfates (7126.1 or 7131.0 eV) for 300 s. At 7126.1 eV, a progressive increase in fluorescence intensity would correspond to the conversion of Fe^{III} to Fe^{II} (and *vice versa*), while at 7131.0 eV, a progressive increase in fluorescence intensity would correspond to the conversion of Fe^{II} to Fe^{III} (and *vice versa*).

during preparation, either for standard compounds or for highly hydrated plant tissues (Fig. 2).

4. Discussion

Our current study has demonstrated the photoreduction of Fe^{III} during X-ray analysis of standards and (to a much lesser extent) plant tissues during an experiment investigating the speciation of Fe in tissues of rice. These findings in regard to the photoreduction of Fe^{III} are in agreement with the data reported previously. For example, Terzano *et al.* (2013) found photoreduction of Fe^{III} when examining Fe in hydrated plant sap at the Fe *K* edge, with these authors reporting a photon flux of *ca* 1×10^{12} (similar to the present study) by comparing XANES spectra following exposure for 1, 5 and 10 XANES scans, corresponding to 600, 3000 and 6000 s exposure in their experimental system. Similarly, using soft X-rays at the Fe *L* edge, George *et al.* (2008) examined metalloproteins, finding rapid photoreduction of Fe^{III} to Fe^{II}. Furthermore, Gonçalves Ferreira *et al.* (2013) examined an inorganic substrate (soda-lime silicate glass), finding photoreduction of Fe^{III} caused by the X-ray beam at the Fe *K* edge during analysis at room temperature.

Importantly, our study has provided conditions that are suitable for preserving Fe speciation and minimizing the extent of beam damage during analysis. Specifically, we demonstrate that although the use of highly hydrated samples for the analysis of Fe speciation can result in large changes in Fe speciation caused by beam damage, the freeze-drying process largely prevented this photoreduction and caused only comparatively small changes in the XANES spectra. This is important, given the crucial roles of Fe within soil–plant systems. Freeze drying also has the advantage of increasing the concentrations of absorbers, which is important in experiments using dilute samples (such as plant tissues) (George *et al.*, 2012).

Although we recommend in the present study that samples should be freeze dried prior to XAS analyses for Fe, we are not recommending that this be standard practice in all biological experiments. For example, using the present experimental setup at the XAS beamline of the Australian Synchrotron, we have previously found that the use of hydrated (frozen) plant tissues to examine a range of metal(loid)s did not result in beam damage when examining Zn (Kopittke *et al.*, 2011), Mn (Kopittke *et al.*, 2013), Ag (Wang *et al.*, 2015) and Cd (Cheng *et al.*, 2016). Nevertheless, Fe is not the only element for which photoreduction has been observed. For example, in plant tissues, photoreduction has also been reported for As (Lombi *et al.*, 2011), Se (Wang *et al.*, 2013) and Cu (Yang *et al.*, 2011). Thus, we contend that it is imperative that studies examining biological samples at XAS beamlines conduct preliminary studies to investigate whether beam damage is occurring. Where no beam damage is evident, the use of hydrated (frozen) samples is generally the preferred option. Instead, freeze drying of samples should only be considered where beam damage is evident, such as in the current study where we examined Fe, which is particularly redox sensitive.

It is also important to note that, in some instances, freeze drying may not be the preferred method of sample preparation. For example, if the primary interest of a study is to

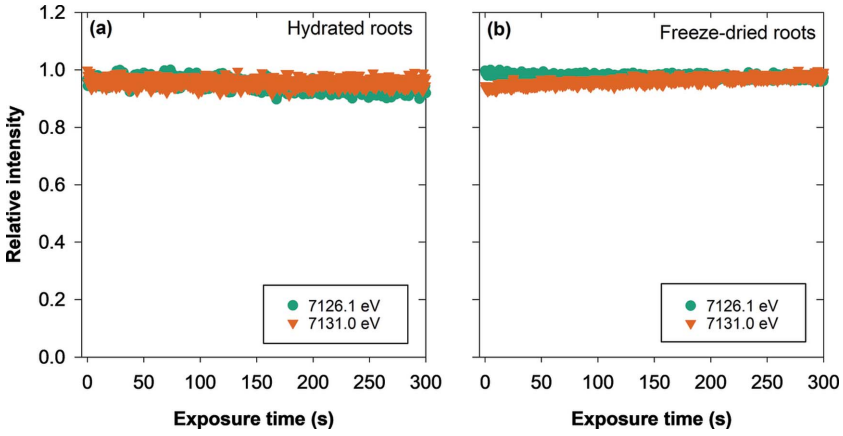

Figure 5
Changes in Fe speciation in roots of rice, either (*a*) hydrated or (*b*) freeze-dried roots, following growth in 25 μ*M* Fe^{III} EDTA for 7 days (Experiment 5). Samples were scanned at constant energy corresponding to the white line peaks of Fe^{II} and Fe^{III} sulfates (7126.1 or 7131.0 eV) for 300 s. At 7126.1 eV, a progressive increase in fluorescence intensity would correspond to the conversion of Fe^{III} to Fe^{II} (and *vice versa*), while at 7131.0 eV, a progressive increase in fluorescence intensity would correspond to the conversion of Fe^{II} to Fe^{III} (and *vice versa*).

determine the ligand to which Fe is bound rather than determining the oxidation state of the Fe, then freeze drying may not necessarily be the most suitable approach. This is because it is possible that strong ligands may remain bound to Fe even if the oxidation state of Fe changes. However, it is possible that sample-preparation techniques (such as freeze drying) may alter the ligand to which Fe is bound despite maintaining its oxidation state, thereby causing experimental artefacts. Thus, careful consideration must always be given to the experimental system and the nature of the information required.

In the present study, we have focused on changes in the sample environment (freeze drying) as a method for limiting beam damage. It is also possible sometimes to take other precautions in order to reduce beam damage, including by altering properties of the beamline itself. For example, George *et al.* (2012) identifies that damage can be reduced by decreasing the X-ray beam flux density, the use of cryogenic temperatures, sample translation, use of a photon shutter to reduce X-ray exposure and the use of electrochemical XAS cells. Such approaches should also be considered and implemented where possible. However, in the present study, despite defocusing the beam to the maximum possible as well as using a cryostat (*ca* 12 K) for all samples, rapid photoreduction was still observed. Thus, a multi-faceted approach is likely to be required in such experiments.

We also observed that the ligand alters the rate of photoreduction of Fe^{III}, with this being in agreement with previous reports. For example, Abrahamson *et al.* (1994) examined photosensitivity of a range of Fe-containing samples complexed with carboxylic acids, finding that photoreduction of Fe^{III} to Fe^{II} decreased in the order: oxalate > tartate > citrate > malate > isocitrate. In a similar manner, Terzano *et al.* (2013) found that whilst Fe^{III} was photoreduced when complexed with succinate, nicotianamine and α-ketoglutarate, it was not photoreduced when complexed with citrate, acetate, malate, shikimate or fumarate – results which differ somewhat from the present study.

In the present study, we have examined speciation of Fe in bulk plant tissues at an XAS beamline. However, speciation can also be examined using μ-XANES at XFM beamlines. In such analyses, XANES spectra are often collected from samples at room temperature, with the samples also often hydrated. Thus, for such analyses, considerable care is required to avoid the photoreduction of Fe. It is noteworthy in this regard that fast fluorescence detector systems at XFM beamlines are now allowing 'fluorescence XANES imaging' (Kopittke *et al.*, 2014). In this approach, XANES spectra can potentially be extracted from every pixel in the map. Importantly, given that the total dwell can be in the range of <1 s per pixel (Blamey *et al.*, 2015; Kopittke *et al.*, 2014), this approach is potentially of value for overcoming issues of photoreduction of redox-sensitive metal(loid)s.

It must be noted that in the present study we have only examined Fe^{II} and Fe^{III} (with these being the most environmentally relevant forms of Fe), but other studies have previously found that Fe^{0} and Fe^{I} can potentially photooxidize in soft X-ray beams (George *et al.*, 2008). Finally, the issue of radiation damage and experimental artefacts is also not limited to XAS analyses. For example, using X-ray crystallography to examine proteins, Weik *et al.* (2000) also demonstrated problems with radiation damage. Specifically, these authors demonstrated cleavage of disulfide bridges and loss of definition of carboxyl groups of acidic residues, with these authors also using a third-generation synchrotron with a photon flux of 5×10^{12} photons s^{-1} through a collimator 0.15 mm in diameter.

In conclusion, our data demonstrate how to minimize the likelihood of beam damage during X-ray analyses of Fe speciation in plant tissues, with only comparatively small differences between the use of freeze-dried samples and highly hydrated samples in regard to Fe speciation analysis. However, substantial differences were observed in the rate of photoreduction, depending upon the coordination chemistry of the Fe as well as the properties of the samples themselves (for example, hydrated standards compared with hydrated plant tissues). Thus, whilst we have shown that studies should always give consideration to the potential formation of beam damage, care must also be taken to ensure that the most sensitive samples are examined when assessing the impact of beam damage. Where beam damage cannot be reduced through altering sample conditions, consideration should also be given to altering the conditions of the beamline. For example, it may be possible to reduce flux density, either by increasing beam size or by decreasing total flux. Also, consideration should be given to conducting multiple shorter scans in different parts of the sample which can then be

averaged to yield a single spectrum. It is important to note that the configuration of each individual X-ray beamline is important and will influence the magnitude of the beam damage observed. Finally, for studies examining metal(loid)s which are less redox sensitive than Fe, it is likely that the freeze drying of samples is not required, with this being preferable as the freeze-drying process itself could potentially cause experimental artefacts in some situations. Indeed, it is our hope that our work will encourage others to explicitly examine issues of beam damage within their experimental systems and thereby take steps to avoid these potential problems. In the present study, we show that even if beam damage occurs within seconds or minutes of exposure, this can be assessed by examining fluorescence intensity at a constant energy over time.

Acknowledgements

This research was undertaken on the XAS beamline at the Australian Synchrotron, part of ANSTO (Australian Nuclear Science and Technology Organisation).

Funding information

This work was supported by the Natural Science Foundation of China (grant No. 21661132001 and 41671309), the Innovative Research Team Development Plan of the Ministry of Education of China (grant No. IRT_17R56) and the fundamental research funds for the central universities of China (grant No. KYT201802 and No. KYT201624).

References

Abrahamson, H. B., Rezvani, A. B. & Brushmiller, J. G. (1994). *Inorg. Chim. Acta*, **226**, 117–127.
Bai, Y., Yang, T., Liang, J. & Qu, J. (2016). *Water Res.* **98**, 119–127.
Blamey, F. P. C., Hernandez-Soriano, M. C., Cheng, M., Tang, C., Paterson, D. J., Lombi, E., Wang, W. H., Scheckel, K. G. & Kopittke, P. M. (2015). *Plant Physiol.* **169**, 2006–2020.
Burton, E. D., Bush, R. T., Sullivan, L. A., Hocking, R. K., Mitchell, D. R. G., Johnston, S. G., Fitzpatrick, R. W., Raven, M., McClure, S. & Jang, L. Y. (2009). *Environ. Sci. Technol.* **43**, 3128–3134.
Castillo-Michel, H. A., Larue, C., Pradas del Real, A. E., Cotte, M. & Sarret, G. (2017). *Plant Physiol. Biochem.* **110**, 13–32.
Cheng, M., Wang, P., Kopittke, P. M., Wang, A., Sale, P. W. G. & Tang, C. (2016). *J. Exp. Bot.* **67**, 5041–5050.
De Brier, N., Gomand, S. V., Donner, E., Paterson, D., Smolders, E., Delcour, J. A. & Lombi, E. (2016). *Plant Cell Environ.* **39**, 1835–1847.
Doong, R. & Schink, B. (2002). *Environ. Sci. Technol.* **36**, 2939–2945.
Essilfie-Dughan, J., Hendry, M. J., Dynes, J. J., Hu, Y., Biswas, A., Lee Barbour, S. & Day, S. (2017). *Sci. Total Environ.* **586**, 753–769.
George, G. N., Pickering, I. J., Pushie, M. J., Nienaber, K., Hackett, M. J., Ascone, I., Hedman, B., Hodgson, K. O., Aitken, J. B., Levina, A., Glover, C. & Lay, P. A. (2012). *J. Synchrotron Rad.* **19**, 875–886.
George, S. J., Fu, J., Guo, Y., Drury, O. B., Friedrich, S., Rauchfuss, T., Volkers, P. I., Peters, J. C., Scott, V., Brown, S. D., Thomas, C. M. & Cramer, S. P. (2008). *Inorg. Chim. Acta*, **361**, 1157–1165.
Gonçalves Ferreira, P., de Ligny, D., Lazzari, O., Jean, A., Cintora Gonzalez, O. & Neuville, D. R. (2013). *Chem. Geol.* **346**, 106–112.
Grillet, L., Ouerdane, L., Flis, P., Hoang, M. T. T., Isaure, M.-P., Lobinski, R., Curie, C. & Mari, S. (2014). *J. Biol. Chem.* **289**, 2515–2525.
Hayes, S. M., Root, R. A., Perdrial, N., Maier, R. M. & Chorover, J. (2014). *Geochim. Cosmochim. Acta*, **141**, 240–257.
Heyden, B. P. von der, Hauser, E. J., Mishra, B., Martinez, G. A., Bowie, A. R., Tyliszczak, T., Mtshali, T. N., Roychoudhury, A. N. & Myneni, S. C. B. (2014). *Environ. Sci. Technol. Lett.* **1**, 387–392.
James, S. A., Hare, D. J., Jenkins, N. L., de Jonge, M. D., Bush, A. I. & McColl, G. (2016). *Sci. Rep.* **6**, 20350.
King, D. W. (1998). *Environ. Sci. Technol.* **32**, 2997–3003.
Kopittke, P. M., de Jonge, M. D., Wang, P., McKenna, B. A., Lombi, E., Paterson, D. J., Howard, D. L., James, S. A., Spiers, K. M., Ryan, C. G., Johnson, A. A. T. & Menzies, N. W. (2014). *New Phytol.* **201**, 1251–1262.
Kopittke, P. M., Lombi, E., McKenna, B. A., Wang, P., Donner, E., Webb, R. I., Blamey, F. P. C., de Jonge, M. D., Paterson, D., Howard, D. L. & Menzies, N. W. (2013). *Physiol. Plant.* **147**, 453–464.
Kopittke, P. M., Menzies, N. W., de Jonge, M. D., McKenna, B. A., Donner, E., Webb, R. I., Paterson, D. J., Howard, D. L., Ryan, C. G., Glover, C. J., Scheckel, K. G. & Lombi, E. (2011). *Plant Physiol.* **156**, 663–673.
Lombi, E., Scheckel, K. G. & Kempson, I. M. (2011). *Environ. Exp. Bot.* **72**, 3–17.
Marschner, H. & Römheld, V. (1994). *Plant Soil*, **165**, 261–274.
Morgan, K. E., Burton, E. D., Cook, P., Raven, M. D., Fitzpatrick, R. W., Bush, R., Sullivan, L. A. & Hocking, R. K. (2009). *J. Phys. Conf. Ser.* **190**, 012144.
Prietzel, J., Thieme, J., Eusterhues, K. & Eichert, D. (2007). *Eur. J. Soil Sci.* **58**, 1027–1041.
Ravel, B. & Newville, M. (2005). *J. Synchrotron Rad.* **12**, 537–541.
Shorttle, O., Moussallam, Y., Hartley, M. E., Maclennan, J., Edmonds, M. & Murton, B. J. (2015). *Earth Planet. Sci. Lett.* **427**, 272–285.
Sigfridsson, K. G. V., Chernev, P., Leidel, N., Popović-Bijelić, A., Gräslund, A. & Haumann, M. (2013). *J. Biol. Chem.* **288**, 9648–9661.
Sposito, G. (2008). *The Chemistry of Soils*, 2nd ed., p. 329. New York: Oxford University Press.
Terzano, R., Mimmo, T., Vekemans, B., Vincze, L., Falkenberg, G., Tomasi, N., Schnell Ramos, M., Pinton, R. & Cesco, S. (2013). *Anal. Bioanal. Chem.* **405**, 5411–5419.
Wang, P., Lombi, E., Sun, S., Scheckel, K. G., Malysheva, A., McKenna, B. A., Menzies, N. W., Zhao, F. J. & Kopittke, P. M. (2017). *Environ. Sci. Nano*, **4**, 448–460.
Wang, P., Menzies, N. W., Chen, H., Yang, X., McGrath, S. P., Zhao, F. J. & Kopittke, P. M. (2018). *Environ. Sci. Technol.* **52**, 4901–4909.
Wang, P., Menzies, N. W., Lombi, E., McKenna, B. A., de Jonge, M. D., Paterson, D. J., Howard, D. L., Glover, C. J., James, S., Kappen, P., Johannessen, B. & Kopittke, P. M. (2013). *Plant Physiol.* **163**, 407–418.
Wang, P., Menzies, N. W., Lombi, E., Sekine, R., Blamey, F. P. C., Hernandez-Soriano, M. C., Cheng, M., Kappen, P., Peijnenburg, W. J. G. M., Tang, C. & Kopittke, P. M. (2015). *Nanotoxicology* **9**, 1041–1049.
Weik, M., Ravelli, R. B. G., Kryger, G., McSweeney, S., Raves, M. L., Harel, M., Gros, P., Silman, I., Kroon, J. & Sussman, J. L. (2000). *Proc. Natl Acad. Sci. USA*, **97**, 623–628.
Wilke, M., Farges, F., Petit, P.-E., Brown, G. E. Jr & Martin, F. (2001). *Am. Mineral.* **86**, 714–730.
Wu, Y., Kukkadapu, R. K., Livi, K. J. T., Xu, W., Li, W. & Sparks, D. L. (2018). *ACS Earth Space Chem.* **2**, 256–268.
Yang, J., Regier, T., Dynes, J. J., Wang, J., Shi, J., Peak, D., Zhao, Y., Hu, T., Chen, Y. & Tse, J. S. (2011). *Anal. Chem.* **83**, 7856–7862.
Yoshimura, E., Sakaguchi, T., Nakanishi, H., Nishizawa, N. K., Nakai, I. & Mori, S. (2000). *Phytochem. Anal.* **11**, 160–162.